PLOS ONE

RESEARCH ARTICLE

Pupil responses to hidden photoreceptor–specific modulations in movies

Manuel Spitschan[1,2,3]*, **Marina Gardasevic**[4], **Franck P. Martial**[4], **Robert J. Lucas**[4], **Annette E. Allen**[4]

1 Department of Experimental Psychology, University of Oxford, Oxford, United Kingdom, **2** Centre for Chronobiology, Psychiatric Hospital of the University of Basel, Basel, Switzerland, **3** Transfaculty Research Platform Molecular and Cognitive Neurosciences, University of Basel, Basel, Switzerland, **4** Division of Neuroscience & Experimental Psychology, Faculty of Biology, Medicine and Health, University of Manchester, Manchester, United Kingdom

* manuel.spitschan@psy.ox.ac.uk

Citation: Spitschan M, Gardasevic M, Martial FP, Lucas RJ, Allen AE (2019) Pupil responses to hidden photoreceptor–specific modulations in movies. PLoS ONE 14(5): e0216307. https://doi.org/10.1371/journal.pone.0216307

Editor: Tudor C Badea, National Eye Centre, UNITED STATES

Received: February 13, 2019

Accepted: April 17, 2019

Published: May 9, 2019

Data Availability Statement: All data and code to perform the data analyses reported here can be found at https://github.com/spitschan/Spitschan2019_PLOSONE.

Funding: This work was supported by a Sir Henry Wellcome Trust Fellowship (Wellcome Trust 204686/Z/16/Z to MS); a Junior Research Fellowship Travel Grant from Linacre College, University of Oxford (MS); a Dean's Prize Fellowship (Faculty of Biology Medicine and Health, University of Manchester to AEA); the European Research Council (268970) and a Wellcome Trust

Abstract

Under typical daytime light levels, the human pupillary light response (PLR) is driven by the activity of the L, M, and S cones, and melanopsin expressed in the so-called intrinsically photosensitive retinal ganglion cells (ipRGCs). However, the importance of each of these photoreceptive mechanisms in defining pupil size under real-world viewing conditions remains to be established. To address this question, we embedded photoreceptor-specific modulations in a movie displayed using a novel projector-based five-primary spatial stimulation system, which allowed for the precise control of photoreceptor activations in time and space. We measured the pupillary light response in eleven observers, who viewed short cartoon movies which contained hidden low-frequency (0.25 Hz) silent-substitution modulations of the L, M and S cones (no stimulation of melanopsin), melanopsin (no stimulation of L, M and S cones), both L, M, and S cones and melanopsin or no modulation at all. We find that all photoreceptors active at photopic light levels regulate pupil size under this condition. Our data imply that embedding modulations in photoreceptor contrast could provide a method to manipulate key adaptive aspects of the human visual system in everyday, real-world activities such as watching a movie.

Introduction

Photoreception in the human retina proceeds from rods, cones and the photopigment melanopsin, which is expressed in a subset of so-called *intrinsically photosensitive retinal ganglion cells* (ipRGCs) [1–5]. All retinal photoreceptors contribute to visual function, though their exact contributions in naturalistic behaviour depend on the spatial and temporal characteristics of the retinal stimulus [6]. At photopic light levels, pupil size is controlled by an excitatory input of L+M (luminance), an inhibitory input of S cones (and possibly M cones, see [7, 8]), as well as a positive input from melanopsin (Fig 1A), along with small input from rods. Since the pupil, the aperture of the eye, changes its size depending on the activity of the photoreceptors

Investigator Award (078808) both to RJL; and the Manchester MRC Doctoral Training Partnership (supporting MG). The funders had no role in study design, data collection and analysis, decision to publish, or preparation of the manuscript.

Competing interests: The authors have declared that no competing interests exist.

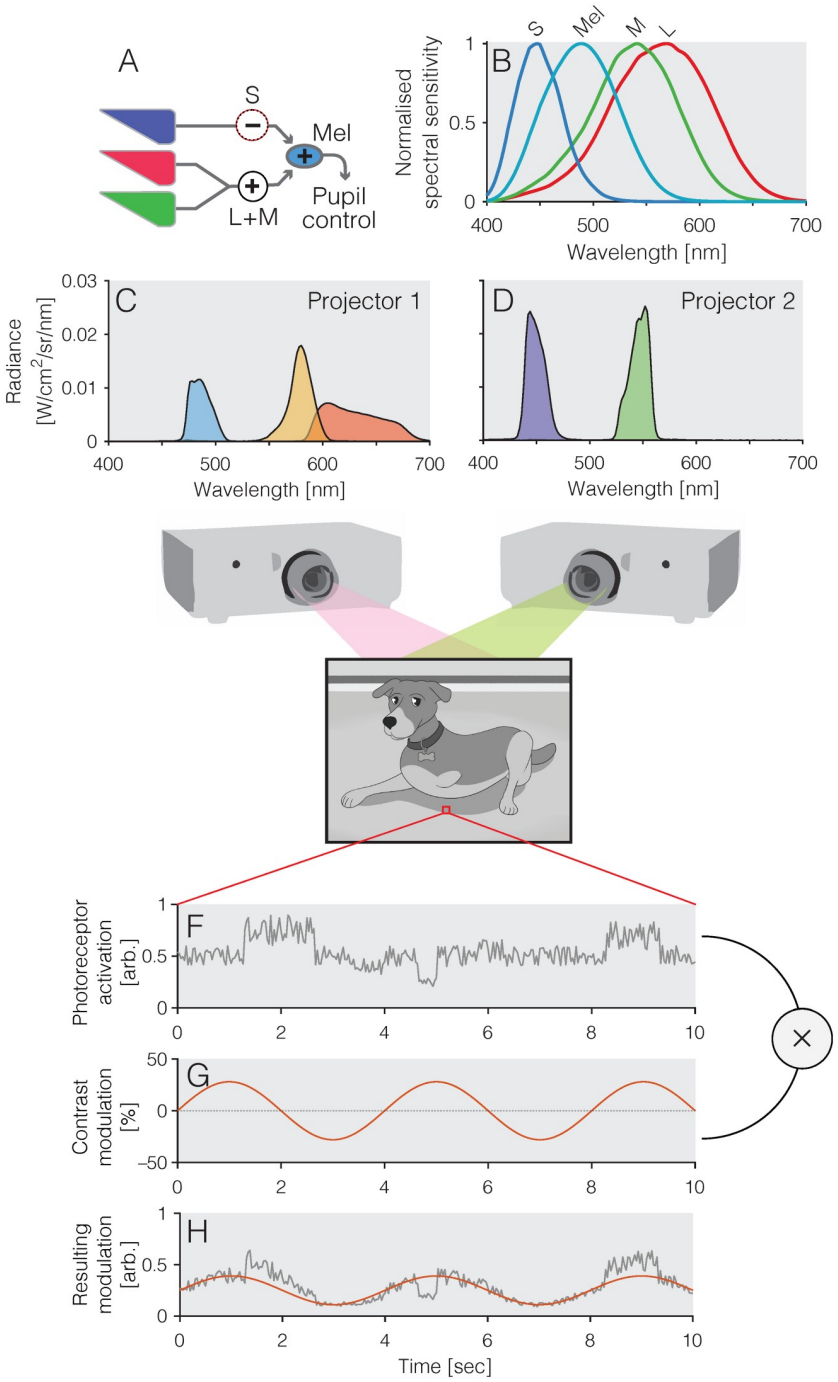

Fig 1. Fundamentals and methods. *A*) Schematic circuit diagram of the human pupillary light response, with L+M cones, and melanopsin, providing an excitatory drive to pupil constriction, and S cones yielding an inhibitory input; *B*) Spectral sensitivities of the human photoreceptors; *C and D*) Spectral radiance of the five primaries for the two projectors; *E*) Frame from cartoon (not from stimulus set); *F*) Sample time course over 10 sec of one pixel of the cartoon, displaying local variations in luminance; *G*) Time course of a pure sinusoidal stimulus (0.25 Hz) stimulating a given photoreceptor class; *H*) The sinusoidal stimulus get superimposed with the variations in pixel luminance so as to yield an embedded sinusoidal modulation while retaining image contrast.

https://doi.org/10.1371/journal.pone.0216307.g001

in the retina, pupillometry represents a non-invasive and convenient method of assessing photoreceptor function.

The contributions of different photoreceptors to pupillary control have been characterised in analytical and parametric studies under well-controlled but rather reduced stimulus conditions typically employing spatially homogenous fields of different visual extent [7–16]. However, under real-world conditions, the importance of each photoreceptor class in defining pupil size remains to be established. In this study, we examined the possibility to address this question by embedding photoreceptor-specific modulations into movies seen under real-world viewing conditions.

In this work, we used a modified projector system, the design of which was described previously [17], to examine the pupil responses to photoreceptor-selective sinusoidal modulations embedded in short greyscale Tom & Jerry cartoon clips. Under photopic conditions, we examined responses to stimuli targeted at the *LMS* cones (with no modulation of melanopsin), *melanopsin* (with no modulation of LMS cones), and a modulation of all photoreceptors to the same extent, which we term *Light Flux*. We find evidence that all photoreceptors regulate pupil size to some degree even during high spatiotemporal frequency modulations.

Methods and materials

Visual stimuli

Stimuli were presented in free-viewing, and participants were free to move their eyes throughout the study. Participants were seated 128 cm from a canvas onto which two spatially aligned projectors projected a movie which contained an embedded 0.25 Hz modulation of photoreceptor contrast enabled by the method silent substitution (see below). The stimulus was a rectangle of dimensions 81 x 109 cm, yielding a total visual angle of approximately 35 x 46 deg^2. The targeted photoreceptors were the LMS cones at equal contrast (*LMS*), melanopsin (*Mel*), or all photoreceptors in unison (*Light Flux*). A fourth condition (*Reference*) contained no modulations. In our low-frequency modulations, we did not control for the effect of cones in the shadow of the retinal blood vessels, so-called penumbral cones, which are known to be stimulated in high-frequency (8–16 Hz) melanopsin-directed modulations [18].

Principle of silent substitution

The spectral tuning of the individual photoreceptors is relatively broadband, and therefore any given light will activate all photoreceptors (Fig 1B). Measurement of downstream responses, such as pupil size, using narrowband, or monochromatic light, will therefore only yield non-specific responses. For example, while in the living human eye, melanopsin will respond maximally to a monochromatic ~488 nm light (the shift from 480 nm of peak pigment absorbance to longer wavelengths due to pre-receptoral filtering by the lens and ocular media), such a light will also activate S cones at ~41%, M cones at ~43%, and L cones at ~26% of their maximal response, respectively. This non-specificity can be overcome by the method of silent substitution [19, 20]. In this method, pairs of spectra are presented to an observer such that the exchange between the spectra only stimulates one class of photoreceptors (the *stimulated* photoreceptors), while not changing the activation of the set of *silenced* photoreceptors. Silent substitution can be achieved using any light source which has at least as many independent lights as spectral photoreceptors under examination, such as sets of LEDs combined optically [7, 9–11, 13–16, 21–23], or combination of broadband light filtered through a diffraction grating and imaged on digital micromirror device [12, 18, 24, 25] (see [26] for technical details), or using modified projectors [17, 27] as in this study.

Projector system

The design of the projector system was first described in [17], but this concrete realization was slightly different. Two 8-bit Hitachi CP-X5022WN 3LCD projectors were stacked on top of each other and the boundaries of their respective projected outputs were aligned by the experimenters using lens adjustment in vertical and horizontal axes, which was further refined with digital cornerstone correction. Alignment was confirmed by visual inspection of corners and edges and in subsequent experiments (not reported here) using high-spatial frequency stimuli. The projectors were modified using optical filters. In Projector 1, the blue primary was modified using a 470 nm cut-off yellow longpass filter (PIXELTEQ, Largo, FL; part # LP470-r40x25x1), making a cyan primary; the green primary was modified using a 463–571 nm notch filter (MidOpt, Palatine, IL; part number #102340892), making yellow. In Projector 2, the blue primary was modified using a 463–571 nm magenta notch filter (MidOpt, Palatine, IL; part #102340892), making violet; and the green primary was modified using a 550 nm bandpass filter (PIXELTEQ, Largo, FL part # Bi550-r40x25x1), producing a narrower green primary. This yielded a dual projector system with five independent primaries (Fig 1C and 1D). At maximum output, the primaries had CIE 1931 *xy* chromaticities: (0.65, 0.34), (0.50, 0.49), (0.08, 0.22), (0.28, 0.70), and (0.16, 0.02), and photopic luminances 54.36, 131.64, 20.84, 185.66, and 8.18 cd/m^2, respectively. The projectors were calibrated and linearised using a CRS SpectroCAL spectrometer (Cambridge Research Systems, Rochester, UK).

Movie stimuli

The movie selected was the Tom & Jerry cartoon "Pent-House Mouse" (1963) [28] (Fig 1E, length 6m11s). The film was first turned into a greyscale movie and then processed in MATLAB to embed photoreceptor-directed modulations into the luminance variations (Fig 1F, 1G and 1H). The photoreceptor contrast of the modulation was 28% for all directions. The modulations were embedded as follows. The (assumed) linear intensity for pixel at position *x*, *y* at time *t* is given by *I(x, y , t)*. The linear 0–1 value for primary *n* (where $n \leq 5$) is then given by:

$$P(x,\ y,\ t; n)\ =\ I(x, y,\ t)\times p_{background} +\ I(x, y,\ t)\times p_{modulation} \times \sin(0.25 \times 2\pi t)$$

The resultant linear values per primary were then converted into 8-bit resolution.

Photoreceptor spectral sensitivities

For the LMS cones, we assumed the physiologically-relevant CIE 2006 photoreceptor sensitivities [29]. Melanopsin spectral sensitivity was derived using the Govardovskii nomogram with λ_{max} = 480 nm, assuming low photopigment density, and applying the same pre-receptoral filtering as for the cones. The receptor spectral sensitivities are available in the Silent Substitution Toolbox (http://github.com/spitschan/SilentSubstitutionToolbox).

Age adjustment

To account for age-dependent differences in pre-receptoral filtering (specifically age-dependent lens-density), stimuli were adjusted in age group for each observer, with discrete categories 20–24 years of age, (22 years reference age) 25–29 years of age (27 years reference age), and 30–34 years of age (32 years of age). Because of the relatively large variability of lens density even across individuals of the same age [30, 31], we reasoned that adjusting according to age group in this way is an acceptable strategy. The age adjustment of pre-receptoral filtering

was performed following the calculations set by the CIE [29]. Within those age groups, lens density does not abruptly change.

Protocol and procedure

After giving informed consent, observers were tested for visual acuity and normal colour vision. Sitting down, they then viewed the four video conditions consecutively, with a two-minute break in between each video. The order of the conditions was randomized between participants. All testing took place during regular daytime working hours (9 to 5 pm).

Pupillometry

The participants' pupil responses were measured using a light-weight binocular eye tracking headset (Pupil Labs GmbH, Berlin, Germany), recording pupil responses at 30 Hz, and also a front-facing view of the participant's view. Using software provided by the manufacturer, 2D ellipses were fit to the resulting videos off-line, and time-locked to the onset of the stimuli using open-source software provided by the manufacturer (https://github.com/pupil-labs/pupil).

Participants

Eleven observers (mean age±SD 24.5±6.5 years, 7 female) were recruited from the wider University of Manchester community. Observers were entered into a raffle to win a hamper. Two participants were authors of this study (A.A. and M.G.). All subjects had 6/5 or better visual acuity (Snellen chart) and normal red-green colour vision as assessed by the Ishihara test [32].

Data analysis

Raw pupil data were processed using custom MATLAB software as follows. Missing data reported from the 2D fitting algorithm were interpreted as eye blinks; to account for transient mis-estimations of the pupil size before and after eye lid closure, we removed additional samples around these events (padding window ±5 samples at 30 Hz). These missing samples were then linearly interpolated. Data were them smoothed with a Savitzky-Golay filter (11^{th} order, frame length 21 samples) using MATLAB's built-in sgolayfilt() function. Raw pupil data (expressed in pixels of the 2D ellipse) were mean-normalised across the entire time series and expressed as percent change around that mean. We then extracted the per-cycle average pupil responses, collapsing across all cycles during the entire cartoon. This per-cycle average was then fit, in a least-squares sense, with a sum of sine and cosine at the stimulation frequency (0.25 Hz); the weights of the sine and cosine were then transformed into amplitude and phase of the evoked pupil response.

Ethics

Ethical approval was obtained from the University of Manchester Ethics commission (approval number #2017-2958-43594359).

Code and data availability

All data and code to perform the data analyses reported here can be found at https://github.com/spitschan/Spitschan2019_PLOSONE.

Results

Photoreceptor-selective modulations embedded in movies produce distinct pupil responses

The 0.25 Hz photoreceptor-specific modulation stimuli evoked distinct responses in all observers (Fig 2A–2D). The strongest response (in amplitude expressed as percent change in pupil diameter relative to the mean) was elicited by the *Light flux* modulations (mean±1SD = 5.0616±1.2554%, median = 5.3051%), followed by *L+M+S* (mean±1SD = 4.1340±0.9263%, median = 4.6839%) (Fig 3A). In many observers we find a small melanopsin-evoked pupil response and in aggregate, there is a significant difference between the *Melanopsin* (mean±1SD = 2.1182±1.3096%, median = 1.5605%) and the *Reference* condition (mean±1SD = 1.0792±0.7652, median = 0.7462%) (Wilcoxon rank sum test, $Z = 2.3639$, $p = 0.0181$). We note that the melanopsin-evoked pupil response is somewhat inconsistent across observers, raising the possibility of individual differences in the observers' melanopsin sensitivity (Figs 2B, 3A and 3B). Though there is nominal difference in mean amplitude between the *Light flux* and the *L+M+S* modulation, this difference is not statistically significant (Wilcoxon rank sum test, $Z = 1.7730$, $p = 0.0762$).

Amplitude and phase of pupil responses

Expressed as amplitude and phase, we find that LMS and light flux pupil responses are well above the noise floor defined by the aggregate fit of the pupil response to the stimulus containing no stimulus at the modulation frequency (0.25 Hz). For all observers, the phase of the LMS and light flux response is delayed relative to the stimulus onset (Figs 2A, 2C and 3B), which is consistent with the "dead time" of the human pupil response (~200–300 msec), i.e. the minimum delay between a stimulus and a pupil response. For the melanopsin-evoked pupil response, we find variability in both amplitude and phase (Figs 2B, 3A and 3B), which warrants further investigation. For some observers and in the group mean data, it even appears as though there is a phase advance in the melanopsin stimulus (positive phase values, Fig 3B). We note that this might well be a very long phase delay consistent with the slow signaling properties of the melanopsin-encoded ipRGC response. We cannot address this in our data, as we focused only on one frequency for the embedded contrast modulations.

Summation of pupil responses

We examined to what extent the sum of the responses to the *LMS* and *Mel* stimuli resembles the response to the *Light Flux* stimulus, which is, when expressed in contrast, the sum of the *LMS* and *Mel* stimuli in the stimulus domain: The *Light Flux* stimulus modulates the L, M, and S cones in the same way that the LMS modulation does; and it modulates melanopsin in the same way that the *Mel* modulation does. We applied a simple linear model by adding the amplitude and phase, expressed as complex sum, of the *LMS* and *Mel* responses, and reading out the amplitude again (Fig 4). Conceptually, this is a vector sum model, where the pupil response to each modulation corresponds to a vector (defined by a given phase and amplitude), and we simply add vectors (Fig 4, inset), yielding a new vector. We find that the amplitude of the complex sum of the *LMS* and *melanopsin* pupil response can account for the *Light Flux* pupil response while the *LMS* response only does so in a limited way (Fig 4). We note that a better fit of the amplitude of the complex sum already requires that the phase of the two summands is aligned in such a way as to yield a better-fitting amplitude, we did not consider the goodness-of-fit of phase.

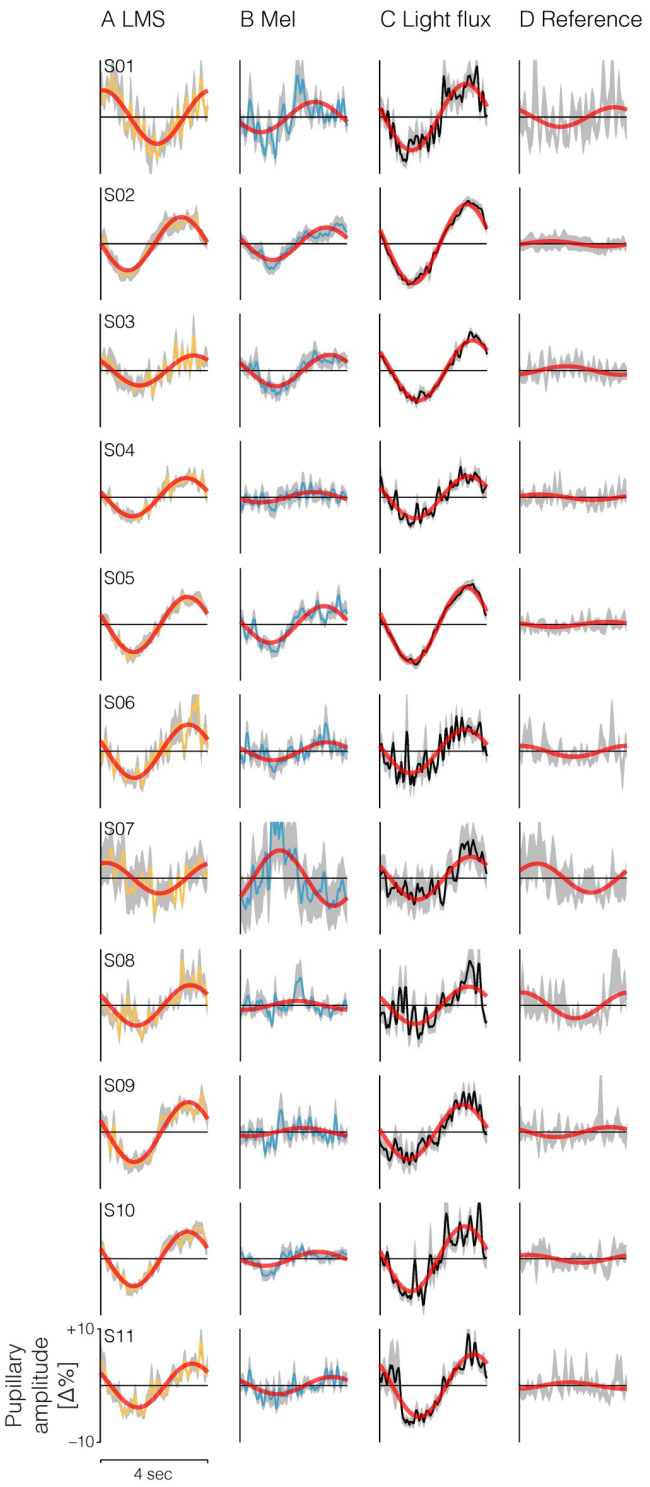

Fig 2. Individual subject pupil data. Data are collapsed (column-wise) across stimulus types. A) L+M+S, B) Melanopsin (*Mel*), C) Light flux (all photoreceptors are modulated), D) no modulation. Red lines indicate the least-squares fit of a sum and cosine at the modulation frequency to cycle-average response.

https://doi.org/10.1371/journal.pone.0216307.g002

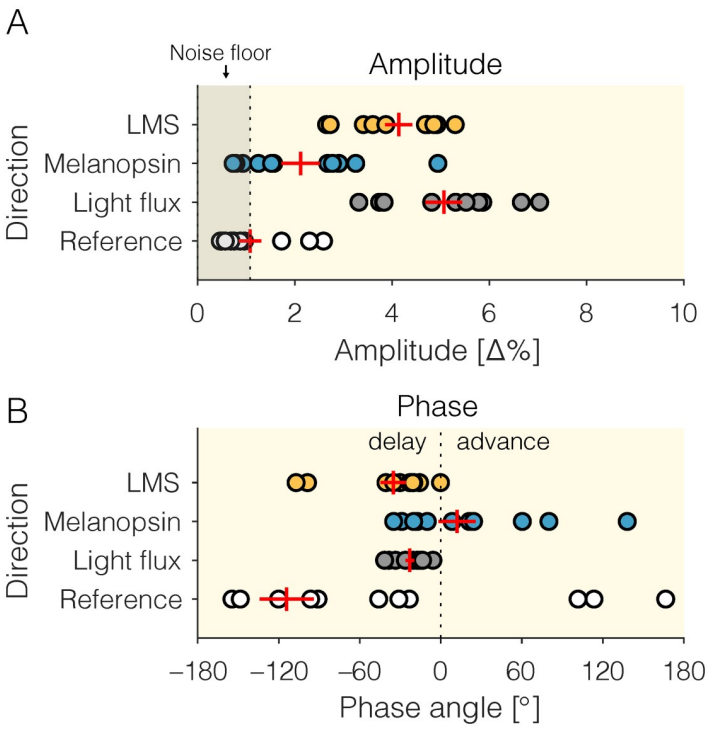

Fig 3. Extracted response properties of the pupil responses to photoreceptor-directed modulations embedded in a cartoon movie. (*A*—amplitude, *B*—phase). Data shown as red crosses are represent mean±SEM across participants. *A*) Amplitude results. Noise floor is given by the mean amplitude of the fitted pupil response to the *Reference* modulations, which contained no additional power at the stimulation frequency. *B*) Phase data, with negative angles corresponding to a phase delay (pupil response lags behind the stimulus), and positive angles corresponding to a phase advance (pupil response precedes the stimulus). Because of the nature of phase, a very long phase delay (longer than –180˚) may manifest as an apparent phase advance as the phase wraps around. The amplitude and phase data shown here correspond directly to the red fit lines in Fig 2.

https://doi.org/10.1371/journal.pone.0216307.g003

Discussion

Summary of results

Pupillary responses to melanopsin-directed stimuli using the method of silent substitution have been documented in the literature [7–16, 24], including by the authors [12, 24]. These studies typically have employed very carefully controlled artificial stimuli. However, past work has not addressed the question of how these photoreceptors each define pupil size during natural viewing. In this study, we find that by embedding photoreceptor-selective modulations in cartoon movie stimuli viewed under real-world conditions, we can elicit pupil responses specific to the receptor type. Consistent with what we would predict from studies employing spatially homogenous stimuli, we find a subtle but significant response to the melanopsin-mediated stimulus at the stimulation frequency (0.25 Hz). The response to the *Light flux* modulation is in mean amplitude larger than the response to the *LMS* modulation (though not statistically significant), providing some evidence that our paradigm may detect melanopsin contributions in the *Light flux* modulation. Further, we find that we can model the pupil response to the *Light flux* modulation as the complex sum of the responses to the *Melanopsin* and the *LMS* modulation, which is corroborated by an earlier finding [12] (see their Fig S8). We note that using our paradigm, we cannot determine the site of this integration process.

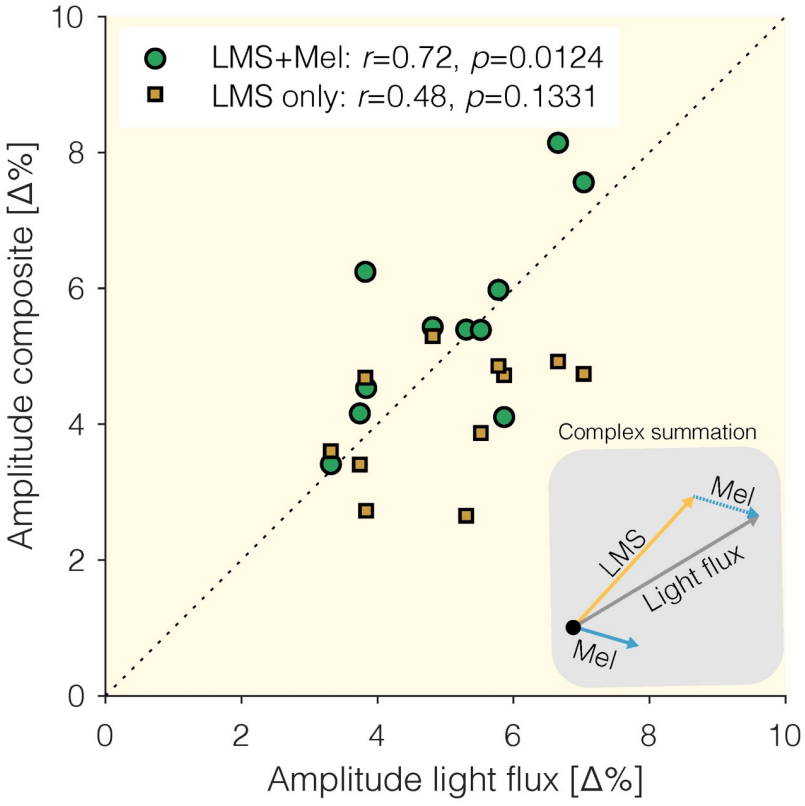

Fig 4. Linear summation model. We compare the amplitude of the pupil response to the *Light flux* modulation to the amplitude of two candidate models: The response to the *LMS* modulation, and the complex sum of the response to the *LMS* modulation and the response to the *Mel* modulation. *Inset*: Visualization of the vector summation model.

https://doi.org/10.1371/journal.pone.0216307.g004

Defining pupil size during free viewing of movie stimuli under real-world conditions

By embedding the modulations in an "entertainment" movie, we have placed the task in an ecologically-relevant context for using a video display unit (VDU). Allowing the participants to freely view the movie and not adhere to specific fixation procedures gives the paradigm an additional real-world aspect. While much emphasis has been placed on examining the photoreceptor inputs into pupillary control under well-controlled but relatively reduced stimulus conditions, our approach provides an understanding of these inputs that is complementary to more parametric and analytical approaches. Using this pragmatic approach to see if we could modulate the activity of photoreceptors in a task that human participants might engage in, in a normal day-to-day sense, we indeed confirm that all photoreceptors known to be active at photopic light levels (as established in previous studies, e.g. [12, 13]), can be manipulated using modulations embedded in movies which can be watched in real-world conditions.

Uncontrolled factors

We wish to highlight that this study has purposely not accounted for a set of factors known to influence pupil size, on the grounds that the goal of this study was to examine pupil responses in an approximation of real-world conditions. Because of the near triad, vergence eye movements, changes of accommodation, and pupillary response go hand in hand when shifting view from near to far distances [33]. Under the unconstrained viewing conditions employed

in this study, observers were able to move both head and eyes freely, thus introducing pupil changes in pupil diameter unrelated to our experimental parameter under control, photoreceptor contrast. As the stimuli were presented using a projection system in an otherwise dark room, eye movements of any sort could displace high contrast edges between the illuminated part of the canvas and the rest of the (dark) wall, which could lead to a transient signal. Because the modulation of contrast was uncorrelated with changes in movie content (and indeed, agnostic to it) which might have elicited gaze shifts, we feel confident that any effects of accommodation and vergence on pupil size average out, as evidence by the flat pupil response in the reference condition. Changes in autonomic arousal, which leads to differences in pupil size [34], might have occurred during the study, which was addressed by counterbalancing the order stimulus conditions.

Data variability

We note that there appears to be large variability in the data. These could reflect individual differences, though this is not explicitly addressed in our data. The variability in the melanopsin response, both in amplitude and phase, warrants further investigation.

Challenges to silent substitution

The silent substitution nominally allows selective stimulation of a given photoreceptor class. Silent substitution requires, however, a good estimate of the human participants' spectral sensitivities. In practice, these are assumed based on standard cone fundamentals such as the physiologically-relevant CIE cone fundamentals [29]; some investigators also allow for an individual-observer calibration routine (e.g. [9–11, 13, 23]). In this work, for practical and pragmatic reasons, we forwent calibration at the level of the individual observer, and simply accounted for age-dependent differences in pre-receptoral filtering, which largely affects the amount of short-wavelength filtering, within a given age bracket spanning 5 years.

In our modulations, we did not account for the potential intrusion of rods at daylight levels. It is generally thought that rods do not participate in visual function at photopic light levels [35, 36]. There are some suggestions that rod saturation might not be complete [37, 38]. In mice, there is also evidence that rods retain the capability to signal at daylight light levels [39, 40]. Generating melanopsin-isolating stimuli to test the hypothesis that rods may be at play at daylight levels requires a severe reduction in melanopsin-isolating contrast [41]. In our data, while we cannot rule out a small rod contribution at the nominally rod-saturating light levels, we think that it is unlikely that the contributions we measured are due to rods as their signals would be heavily reduced at the photopic light levels we used. We also note that if rods were considered to contribute to these types of modulations, they would do so in a similar way for any practical application involving VDUs.

Opportunities for translation

Given the broad impact of light on aspects of human physiology and behavior (such as melatonin suppression, circadian phase-shifting and modulation of alertness), the system and paradigm described here to modulate visual responses in a photoreceptor-selective fashion represents an opportunity to modulate these while people are engaging in everyday tasks such as movie-watching [17]. One powerful further application in the future could be as a method for low-impact "passive" assessment of photoreceptor health in clinical contexts, specifically in pediatric and geriatric populations.

Towards a revision of colorimetry?

In this study, we have employed a 5-primary projector-based system for silent substitution with spatial control at the pixel level, and controlling the activation of the photoreceptors active at daylight: the cones and the melanopsin-containing ipRGCs. Commercially available VDUs have three primaries, which reflects the fact that human colour vision in photopic light levels is trichromatic. However, this study and a recent one [17] employing a similar system find that non-visual responses can be manipulated with a modified VDU with more than three primaries. Additionally, there is more and more evidence that melanopsin contributes to "classical" visual functions such as the perception of brightness [22, 42], colour [9, 43], space (humans: [9]; mice: [44, 45]), contrast [46, 47], and other visual attributes (humans: [24], mice: [48–50]). It remains an interesting question to what extent the classical colour matching functions, which are the basis of our current cone fundamentals, reflect the activity of melanopsin (though the amount of rod contributions have been discussed extensively [51]). Given the numerous roles of melanopsin in visual perception and in regulating physiology and behavior, and the emergence of tetrachromatic or higher-order primary displays, we expect that colorimetry may need some revisions to account for these effects, visual or non-visual.

Acknowledgments

We wish to thank the EEG Lab at the University of Manchester for allowing us to use their space.

Author Contributions

Conceptualization: Manuel Spitschan, Robert J. Lucas, Annette E. Allen.

Data curation: Manuel Spitschan, Marina Gardasevic.

Formal analysis: Manuel Spitschan.

Funding acquisition: Manuel Spitschan, Robert J. Lucas, Annette E. Allen.

Investigation: Manuel Spitschan, Marina Gardasevic, Annette E. Allen.

Methodology: Manuel Spitschan, Marina Gardasevic, Franck P. Martial, Annette E. Allen.

Project administration: Manuel Spitschan, Marina Gardasevic, Robert J. Lucas.

Resources: Manuel Spitschan, Franck P. Martial, Robert J. Lucas, Annette E. Allen.

Software: Manuel Spitschan.

Supervision: Manuel Spitschan, Robert J. Lucas.

Validation: Manuel Spitschan, Marina Gardasevic.

Visualization: Manuel Spitschan.

Writing – original draft: Manuel Spitschan.

Writing – review & editing: Manuel Spitschan, Marina Gardasevic, Robert J. Lucas, Annette E. Allen.

References

1. Provencio I, Rodriguez IR, Jiang G, Hayes WP, Moreira EF, Rollag MD. A novel human opsin in the inner retina. J Neurosci. 2000; 20(2):600–5. PMID: 10632589
2. Berson DM, Dunn FA, Takao M. Phototransduction by retinal ganglion cells that set the circadian clock. Science. 2002; 295(5557):1070–3. https://doi.org/10.1126/science.1067262 PMID: 11834835

3. Hattar S, Liao HW, Takao M, Berson DM, Yau KW. Melanopsin-containing retinal ganglion cells: architecture, projections, and intrinsic photosensitivity. Science. 2002; 295(5557):1065–70. https://doi.org/10.1126/science.1069609 PMID: 11834834
4. Lucas RJ, Hattar S, Takao M, Berson DM, Foster RG, Yau KW. Diminished pupillary light reflex at high irradiances in melanopsin-knockout mice. Science. 2003; 299(5604):245–7. https://doi.org/10.1126/science.1077293 PMID: 12522249
5. Dacey DM, Liao HW, Peterson BB, Robinson FR, Smith VC, Pokorny J, et al. Melanopsin-expressing ganglion cells in primate retina signal colour and irradiance and project to the LGN. Nature. 2005; 433 (7027):749–54. https://doi.org/10.1038/nature03387 PMID: 15716953
6. Lucas RJ, Peirson SN, Berson DM, Brown TM, Cooper HM, Czeisler CA, et al. Measuring and using light in the melanopsin age. Trends Neurosci. 2014; 37(1):1–9. https://doi.org/10.1016/j.tins.2013.10.004 PMID: 24287308
7. Woelders T, Leenheers T, Gordijn MCM, Hut RA, Beersma DGM, Wams EJ. Melanopsin- and L-cone-induced pupil constriction is inhibited by S- and M-cones in humans. Proc Natl Acad Sci U S A. 2018; 115(4):792–7. https://doi.org/10.1073/pnas.1716281115 PMID: 29311335
8. Murray IJ, Kremers J, McKeefry D, Parry NRA. Paradoxical pupil responses to isolated M-cone increments. J Opt Soc Am A Opt Image Sci Vis. 2018; 35(4):B66–B71. https://doi.org/10.1364/JOSAA.35.000B66 PMID: 29603924
9. Zele AJ, Feigl B, Adhikari P, Maynard ML, Cao D. Melanopsin photoreception contributes to human visual detection, temporal and colour processing. Sci Rep. 2018; 8(1):3842. https://doi.org/10.1038/s41598-018-22197-w PMID: 29497109
10. Barrionuevo PA, Cao D. Luminance and chromatic signals interact differently with melanopsin activation to control the pupil light response. J Vis. 2016; 16(11):29. https://doi.org/10.1167/16.11.29 PMID: 27690169
11. Cao D, Nicandro N, Barrionuevo PA. A five-primary photostimulator suitable for studying intrinsically photosensitive retinal ganglion cell functions in humans. J Vis. 2015; 15(1):15 1 27.
12. Spitschan M, Jain S, Brainard DH, Aguirre GK. Opponent melanopsin and S-cone signals in the human pupillary light response. Proc Natl Acad Sci U S A. 2014; 111(43):15568–72. https://doi.org/10.1073/pnas.1400942111 PMID: 25313040
13. Barrionuevo PA, Nicandro N, McAnany JJ, Zele AJ, Gamlin P, Cao D. Assessing rod, cone, and melanopsin contributions to human pupil flicker responses. Invest Ophthalmol Vis Sci. 2014; 55(2):719–27. https://doi.org/10.1167/iovs.13-13252 PMID: 24408974
14. Tsujimura S, Tokuda Y. Delayed response of human melanopsin retinal ganglion cells on the pupillary light reflex. Ophthalmic Physiol Opt. 2011; 31(5):469–79. https://doi.org/10.1111/j.1475-1313.2011.00846.x PMID: 21645019
15. Vienot F, Bailacq S, Rohellec JL. The effect of controlled photopigment excitations on pupil aperture. Ophthalmic Physiol Opt. 2010; 30(5):484–91. https://doi.org/10.1111/j.1475-1313.2010.00754.x PMID: 20883331
16. Tsujimura S, Ukai K, Ohama D, Nuruki A, Yunokuchi K. Contribution of human melanopsin retinal ganglion cells to steady-state pupil responses. Proc Biol Sci. 2010; 277(1693):2485–92. https://doi.org/10.1098/rspb.2010.0330 PMID: 20375057
17. Allen AE, Hazelhoff EM, Martial FP, Cajochen C, Lucas RJ. Exploiting metamerism to regulate the impact of a visual display on alertness and melatonin suppression independent of visual appearance. Sleep. 2018; 41(8).
18. Spitschan M, Aguirre GK, Brainard DH. Selective stimulation of penumbral cones reveals perception in the shadow of retinal blood vessels. PLoS One. 2015; 10(4):e0124328. https://doi.org/10.1371/journal.pone.0124328 PMID: 25897842
19. Estévez O, Spekreijse H. The "silent substitution" method in visual research. Vision Res. 1982; 22 (6):681–91. PMID: 7112962
20. Estévez O, Spekreijse H. A spectral compensation method for determining the flicker characteristics of the human colour mechanisms. Vision Res. 1974; 14(9):823–30. PMID: 4419261
21. Vartanian G, Wong KY, Ku PC. LED Lights With Hidden Intensity-Modulated Blue Channels Aiming for Enhanced Subconscious Visual Responses. IEEE Photonics J. 2017; 9(3).
22. Brown TM, Tsujimura S, Allen AE, Wynne J, Bedford R, Vickery G, et al. Melanopsin-based brightness discrimination in mice and humans. Curr Biol. 2012; 22(12):1134–41. https://doi.org/10.1016/j.cub.2012.04.039 PMID: 22633808
23. Pokorny J, Smithson H, Quinlan J. Photostimulator allowing independent control of rods and the three cone types. Vis Neurosci. 2004; 21(3):263–7. PMID: 15518198

24. Spitschan M, Bock AS, Ryan J, Frazzetta G, Brainard DH, Aguirre GK. The human visual cortex response to melanopsin-directed stimulation is accompanied by a distinct perceptual experience. Proc Natl Acad Sci U S A. 2017; 114(46):12291–6. https://doi.org/10.1073/pnas.1711522114 PMID: 29087940

25. Spitschan M, Datta R, Stern AM, Brainard DH, Aguirre GK. Human Visual Cortex Responses to Rapid Cone and Melanopsin-Directed Flicker. J Neurosci. 2016; 36(5):1471–82. https://doi.org/10.1523/JNEUROSCI.1932-15.2016 PMID: 26843631

26. MacKinnon N, Stange U, Lane P, MacAulay C, Quatrevalet M. Spectrally programmable light engine for in vitro or in vivo molecular imaging and spectroscopy. Appl Opt. 2005; 44(11):2033–40. PMID: 15835352

27. Bayer FS, Paulun VC, Weiss D, Gegenfurtner KR. A tetrachromatic display for the spatiotemporal control of rod and cone stimulation. J Vis. 2015; 15(11):15. https://doi.org/10.1167/15.11.15 PMID: 26305863

28. Tom And Jerry—Complete Volumes 1–6. Warner Home Video; 2006.

29. CIE. Fundamental chromaticity diagram with physiological axes—Part 1 (Technical Report 170–1). Vienna: Central Bureau of the Commission Internationale de l' Éclairage; 2006.

30. Xu J, Pokorny J, Smith VC. Optical density of the human lens. J Opt Soc Am A Opt Image Sci Vis. 1997; 14(5):953–60. PMID: 9114506

31. Pokorny J, Smith VC, Lutze M. Aging of the human lens. Appl Opt. 1987; 26(8):1437–40. https://doi.org/10.1364/AO.26.001437 PMID: 20454339

32. Ishihara S. Tests for Colour Blindness. Tokyo: Kanehara Shuppen Company; 1977.

33. McDougal DH, Gamlin PD. Autonomic control of the eye. Compr Physiol. 2015; 5(1):439–73. https://doi.org/10.1002/cphy.c140014 PMID: 25589275

34. Loewenfeld IE, Lowenstein O. The pupil: anatomy, physiology, and clinical applications. 1st ed. Ames / Detroit: Iowa State University Press / Wayne State University Press; 1993.

35. Aguilar M, Stiles WS. Saturation of the Rod Mechanism of the Retina at High Levels of Stimulation. Optica Acta: International Journal of Optics. 1954; 1(1):59–65.

36. Adelson EH. Saturation and adaptation in the rod system. Vision Res. 1982; 22(10):1299–312. PMID: 7179751

37. Shapiro AG. Cone-specific mediation of rod sensitivity in trichromatic observers. Invest Ophthalmol Vis Sci. 2002; 43(3):898–905. PMID: 11867613

38. Kremers J, Czop D, Link B. Rod and S-cone driven ERG signals at high retinal illuminances. Doc Ophthalmol. 2009; 118(3):205–16. https://doi.org/10.1007/s10633-008-9159-0 PMID: 19101744

39. Altimus CM, Guler AD, Alam NM, Arman AC, Prusky GT, Sampath AP, et al. Rod photoreceptors drive circadian photoentrainment across a wide range of light intensities. Nat Neurosci. 2010; 13(9):1107–12. https://doi.org/10.1038/nn.2617 PMID: 20711184

40. Tikidji-Hamburyan A, Reinhard K, Storchi R, Dietter J, Seitter H, Davis KE, et al. Rods progressively escape saturation to drive visual responses in daylight conditions. Nat Commun. 2017; 8(1):1813. https://doi.org/10.1038/s41467-017-01816-6 PMID: 29180667

41. Spitschan M, Woelders T. The Method of Silent Substitution for Examining Melanopsin Contributions to Pupil Control. Front Neurol. 2018; 9:941. https://doi.org/10.3389/fneur.2018.00941 PMID: 30538662

42. Zele AJ, Adhikari P, Feigl B, Cao D. Cone and melanopsin contributions to human brightness estimation. J Opt Soc Am A Opt Image Sci Vis. 2018; 35(4):B19–B25. https://doi.org/10.1364/JOSAA.35.000B19 PMID: 29603934

43. Cao D, Chang A, Gai S. Evidence for an impact of melanopsin activation on unique white perception. J Opt Soc Am A Opt Image Sci Vis. 2018; 35(4):B287–B91. https://doi.org/10.1364/JOSAA.35.00B287 PMID: 29603954

44. Allen AE, Storchi R, Martial FP, Bedford RA, Lucas RJ. Melanopsin Contributions to the Representation of Images in the Early Visual System. Curr Biol. 2017; 27(11):1623–32 e4. https://doi.org/10.1016/j.cub.2017.04.046 PMID: 28528909

45. Ecker JL, Dumitrescu ON, Wong KY, Alam NM, Chen SK, LeGates T, et al. Melanopsin-expressing retinal ganglion-cell photoreceptors: cellular diversity and role in pattern vision. Neuron. 2010; 67(1):49–60. https://doi.org/10.1016/j.neuron.2010.05.023 PMID: 20624591

46. Schmidt TM, Alam NM, Chen S, Kofuji P, Li W, Prusky GT, et al. A role for melanopsin in alpha retinal ganglion cells and contrast detection. Neuron. 2014; 82(4):781–8. https://doi.org/10.1016/j.neuron.2014.03.022 PMID: 24853938

47. Sonoda T, Lee SK, Birnbaumer L, Schmidt TM. Melanopsin Phototransduction Is Repurposed by ipRGC Subtypes to Shape the Function of Distinct Visual Circuits. Neuron. 2018; 99(4):754–67 e4. https://doi.org/10.1016/j.neuron.2018.06.032 PMID: 30017393

48. Allen AE, Storchi R, Martial FP, Petersen RS, Montemurro MA, Brown TM, et al. Melanopsin-driven light adaptation in mouse vision. Curr Biol. 2014; 24(21):2481–90. https://doi.org/10.1016/j.cub.2014.09.015 PMID: 25308073

49. Storchi R, Milosavljevic N, Eleftheriou CG, Martial FP, Orlowska-Feuer P, Bedford RA, et al. Melanopsin-driven increases in maintained activity enhance thalamic visual response reliability across a simulated dawn. Proc Natl Acad Sci U S A. 2015; 112(42):E5734–43. https://doi.org/10.1073/pnas.1505274112 PMID: 26438865

50. Storchi R, Bedford RA, Martial FP, Allen AE, Wynne J, Montemurro MA, et al. Modulation of Fast Narrowband Oscillations in the Mouse Retina and dLGN According to Background Light Intensity. Neuron. 2017; 93(2):299–307. https://doi.org/10.1016/j.neuron.2016.12.027 PMID: 28103478

51. Wyszecki G, Stiles WS. Color Science: concepts and methods, quantitative data and formulae. 2nd ed. New York: Wiley; 1982.